# THE PROGRESS IN DESIGN, PREPARATION AND MEASUREMENT OF MLL FOR HEPS*

Shuaipeng Yue[1,2], Bin Ji[1], Ming Li[1], Qingyan Hou[1], Guangcai Chang[1,†]

[1] Institute of High Energy Physics, Chinese Academy of Sciences, 19B Yuquan Road, Beijing, China

[2] University of Chinese Academy of Sciences, 19A Yuquan Road, Beijing, China

## Abstract

The multilayer Laue lens (MLL) is a promising optical element with large numerical aperture and aspect ratio in synchrotron radiation facility. The tilted MLLs are designed for the hard X-ray nano-probe beamline of HEPS. Two MLLs with 63(v)×43(h) μm² aperture and focal spot size of 8.1(v)×8.1(h) nm² at 10 keV are fabricated by a 7-meter-long Laue lens deposition machine. Ultrafast laser etching, dicing and focused ion beam are used to fabricate the multilayer into two-dimensional lenses meeting the requirement of diffraction dynamics. The multilayer grows flat without distortion. The smallest accumulated layer position error is below ±5 nm in the whole area and the root mean square (RMS) error is about 2.91 nm by SEM and image processing. The focusing performance of MLL with actual film thickness is calculated by a method based on the couple wave theory (CWT). The calculated full width at half maximum (FWHM) of focus spot is 8.4×8.2 nm² at 10 keV, which is close to the theoretical result.

## INTRODUCTION

The smaller the spot of X-ray focus, the better the ability to distinguish the structure and composition of the material in a smaller spatial scale. The multilayer Laue lens has a large numerical aperture and depth-width ratio, and theoretically can focus x-rays below 1 nm [1], single-atom testing can be performed. Such high spatial resolution will enable the structure of materials to be studied at a new microscopic scale, effectively filling the gap between x-ray and electron microscopes in spatial resolution, it makes the exploration of the relationship between material structure and function more comprehensive and deepened, so it has been widely studied.

In order to improve the focusing resolution of MLL, a lot of research has been done by international researchers. In 2016, Sasa Bajt et al. carried out the fabrication and testing of wedged MLLs lens and obtained 8.4 nm × 6.8 nm at 16.3 keV [2]. In 2020, Xu et al. developed a MEMS template-based optical device for alignment of two linear MLLs, and realized a two-dimensional focusing spot of 14 nm × 13 nm at 13.6 keV photon energy [3]. In this study, we design and fabricate two MLLs with 63(v)×43(h) μm² aperture and calculate their focus performance at 10 keV.

## DESIGN

The MLL consists of alternating regions made of two different materials. The thickness distribution is similar to that of a Fresnel zone plate (FZP). resulting in a focusing effect. The position of the nth layer of the film is determined by the zone plate formula:

$$x_n^2 = n\lambda f + n^2\lambda^2/4 \qquad (1)$$

where $x_n$ represents the position of the thin film, λ is the wavelength of the X-ray, and f is the focal length of the MLL. Additionally, the thickness of each layer dn can be expressed as follows:

$$d_n = x_n - x_{n-1} \approx \frac{\lambda f}{2x_n} \qquad (2)$$

The MLL used within this study was designed at 10 keV using alternate target sputtering of $WSi_2$ and Si on a substrate. To achieve 8 nm focus spot for High Energy Photon Source (HEPS), the two-dimension focused MLLs are designed as follows (see Table 1).

Table 1: MLL Design Parameter

| MLL@10KeV | Horizontal | Vertical |
|---|---|---|
| Aperture [μm] | 43 | 63 |
| Thickness [nm] | 3.3-15 | 3-14 |
| Layers | 8030 | 13030 |
| Optimum depth [μm] | 3.5 | 3.3 |
| Efficiency | 8.4% | 7.2% |
| Focal length [mm] | 3 | 4 |
| FWHM [nm] | 8 | 8 |
| Tilt angle [mrad] | 7.4 | 8.3 |

The one-dimensional diffraction effect is calculated using the dynamics theory of X-ray diffraction. This was first used by Takagi and Taupin Diffraction (TTD) to describe the wavefront change of X-rays propagating when a crystal is distorted [4]. The MLLs' focusing property near focal plane is calculated using the Fresnel-Kirchhoff diffraction integral as shown in Figures 1 and 2. The intensity distribution of focal spot is shown in Figure 3.
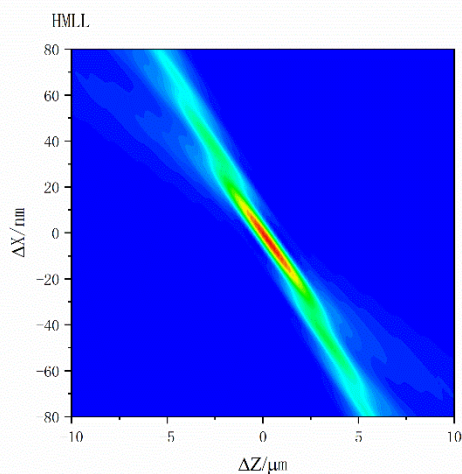
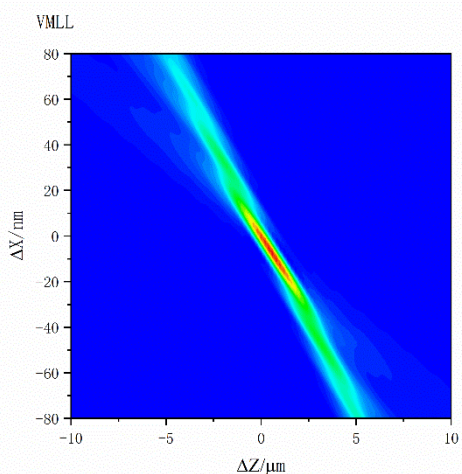Figure 1: The intensity distribution of HMLL near focal plane.



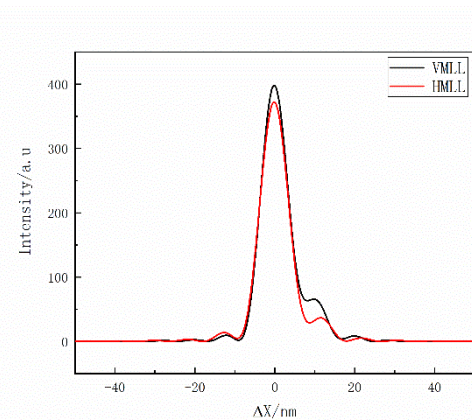Figure 2: The intensity distribution of VMLL near focal plane.



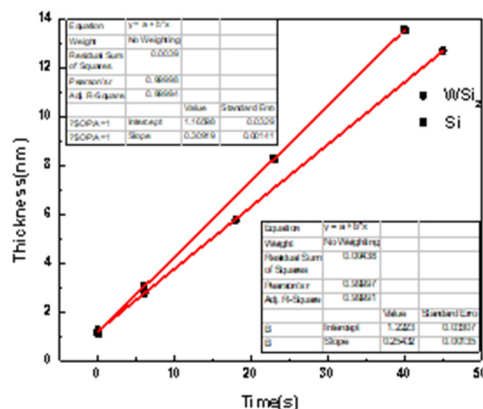Figure 3: The intensity distribution of HMLL and VMLL at focal spot.

## PREPARATION

### Multilayer Preparation

The multilayer is deposited onto a super-polished silicon substrate using a 7-meter-long Laue lens deposition machine with 8 4-inch target. The coating system consists of three parts: (1) load-lock chamber, which can realize the transfer, loading and unloading of samples without destroying the high vacuum of the deposition chamber. (2) testing chamber, on-line measurement of film curvature and stress in the film deposition process. (3) deposition chamber, the target particles are sputtered and deposited on silicon wafer to form multilayer structure mainly by magnetron sputtering technology. The base pressure is below 8E-5 Pa before deposition, and Argon (99.99%) is used as the working gas with a pressure of 0.6 Pa, considering the factors of interface roughness and film stress. The power of the $WSi_2$ target is 40 W, while that of the Si target is 60 W.

The layer thicknesses range of the designed MLLs is varied from 3 nm to 15 nm. Several fixed individual thicknesses within the range are selected to process periodic multilayers to calculate the relationship between individual thickness and deposition time. The X-ray diffractometer (XRD) produced by Bruker D8 advance is used to perform the grazing incidence X-ray reflection (GIXRR) test of the periodic multilayer. The relationship between the thickness of $WSi_2$ and Si and deposition time iss obtained by data fitting as shown in Figure 4.



Figure 4: The relationship between the thickness of $WSi_2$ and Si and deposition time.

The linear fit equation of $WSi_2$ is d = 0.25t+1.22 while that of Si is d = 0.31t+1.17, where d represents the thickness, and t represents the time. In the linear equation, the slope represents the growing rate of individual material, while the intercept represents the thickness when the substrate is moved back and forth above each target. According to the above two equations, the 8030-layer and 13030-layer MLL multilayers are fabricated.

12ᵗʰ Int. Conf. Mech. Eng. Design Synchrotron Radiat. Equip. Instrum.    MEDSI2023, Beijing, China    JACoW Publishing

ISBN: 978-3-95450-250-9        ISSN: 2673-5520        doi:10.18429/JACoW-MEDSI2023-TUOBM05

*Lenses Fabrication*

The incident X-ray energy determines the lens depth along the optical axis to achieve the best efficiency of high numerical aperture focusing. For the MLL designed in Section 2, the optimal depths are determined to be 3.5 µm and 3.3 µm respectively at 10 keV. In order to precisely control the depth of the lenses and to achieve high-quality fine polishing of the entrance and exit surfaces, we use ultra-fast laser etching, dicing, and focused ion beam (FIB) polishing [5].

The multilayer surface is firstly etched by ultra-fast laser equipped with Trumpf ultraviolet femtosecond laser, SCANLAB two-dimensional mirror scanning system and six-axis positioning system produced by PI company. Adjust the sample stage so that the center of the laser focus is located on the surface of the sample. Single-layer etching is started by filling two rectangular patterns in the laser control software, and multiple etching cycles are carried out, so that the etching depth is greater than the total thickness of the MLL, as shown in Figure 5.
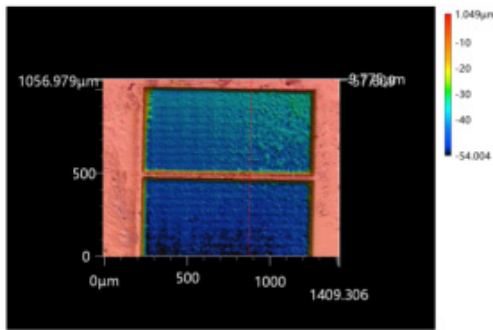


Figure 5: The etching morphology of MLL measured by confocal laser microscope with 10 × lens.

Because the focal length of the MLL is limited (3 ∼ 4 mm), the multilayer after laser etching is cut and separated into small size samples (e. g. 2 mm × 1 mm) by a dicing machine. After that, FIB is carried out to further thin the lenses to the depth along the optical axis that satisfies the diffraction dynamics. It is simultaneously necessary to use FIB to finely polish the entrance and exit surfaces of the MLLs to improve the surface roughness and to reduce scattering of X-rays. The morphology of the final processed lenses under scanning electron microscope (SEM) test is shown in Figure 6.
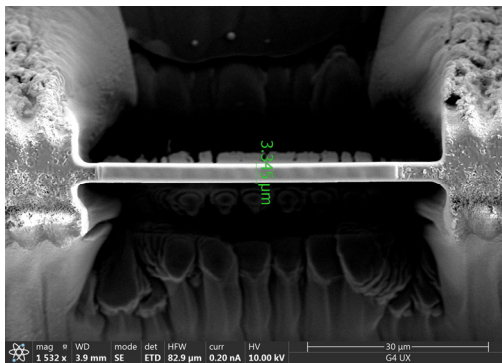


Figure 6: MLL top view measured by SEM.

## CHARACTERIZATION

In order to characterize the processing quality of MLL, the cross-section of the multilayer was observed by Transmission electron microscope (TEM) before the lenses fabrication as shown in Figure 7. The material of dark layer is $WSi_2$, while the light layer represents the Si. It can be seen that multilayer structure is undamaged after deposition. All the layer interfaces stay smooth without distortion.
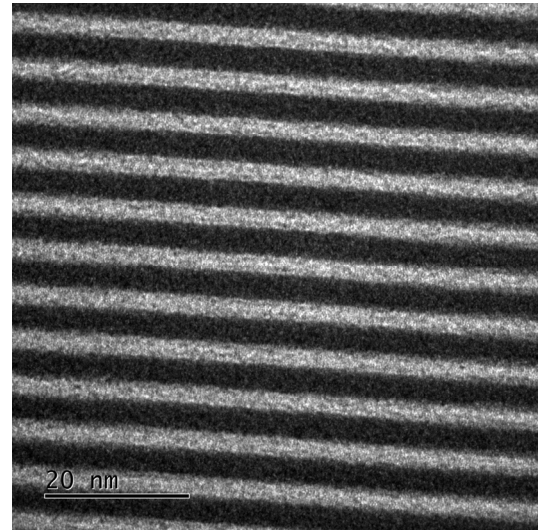


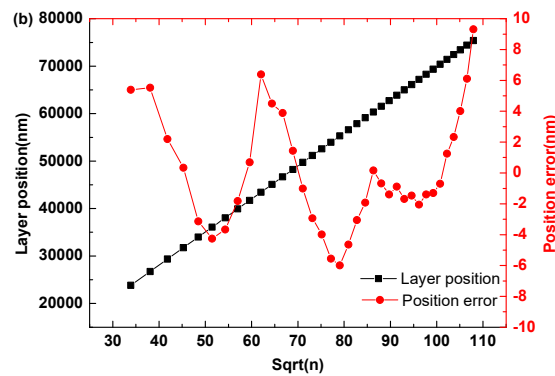Figure 7: Cross-section of the multilayer observed by TEM.
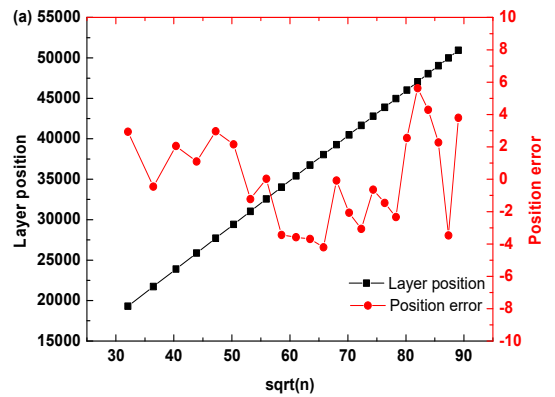


Figure 8: Layer position and position error of HMLL(a) and VMLL(b).

During the preparation of the MLL multilayers, every 300th layer of Si was replaced by $WS_{i2}$ as the marker. The location of each marker layer can be obtained by measuring the thickness of each marker region. In theory, the position of the zone is proportional to the arithmetic square root of the zone number, but the actual marker layer position has a small error that deviates from a linear distribution due to long-term drift of the deposition rate and rate stability, as shown in the Figure 8. The position error of HMLL and VMLL are listed in Table 2.

Table 2: Position Error of HMLL and VMLL

| Position error | PV [nm] | RMS [nm] |
|---|---|---|
| HMLL | < ±4 | 2.91 |
| VMLL | < ±8 | 3.70 |

Ideally, the positions of the layers should adhere to the zone plate law for optimal performance. However, due to a growth-rate error, an additional quadratic term is also present, as evidenced by the best fit to the experimental data. By substituting the actual layer positions measured by the SEM into the central equations for the CWT method for MLLs which are explained in detail elsewhere [6], we can derive a set of differential equations that can be solved numerically. This numerical solution allows us to calculate the wavefront of the diffracted wave on the exit surface of

the MLL. Utilizing the Huygens-Fresnel principle, we can further determine the complex wavefront of the diffracted wave at any point beyond the MLL. The FWHM of the HMLL and VMLL is $8.4×8.2$ nm$^2$, as shown in Figure 9.

## CONCLUSION

In this paper, two MLLs with $63(v)×43(h)$ μm$^2$ aperture and focal spot size of $8.1(v)×8.1(h)$ nm$^2$ at 10 keV are designed by diffraction dynamics and fabricated by a 7-meter-long Laue lens deposition machine. Ultrafast laser etching, dicing and focused ion beam are used to fabricate the multilayer into two-dimensional lenses meeting the requirement of diffraction dynamics. The accumulated layer position errors of HMLL and VMLL are 2.91 nm and 3.70 nm by SEM and image processing. The focusing performance of MLL with actual film thickness is calculated by a method based on CWT. The calculated FWHM of focus spot is $8.4×8.2$ nm$^2$ at 10 keV, which is close to the theoretical result of $8.1×8.1$ nm$^2$. The actual focusing performance of MLLs will be tested when the HEPS nano-probe beamline is mounted.

## REFERENCES

[1] H. Yan, H. Kang, R. Conley, C. Liu, *et al.*, "Multilayer Laue Lens: A Path Toward One Nanometer", *X-Ray Opt. Instr.*, vol. 2010, p. 401854, Dec. 2010.

[2] S. Bajt, M. Prasciolu, H. Fleckenstein, *et al.*, "X-ray focusing with efficient high-NA multilayer Laue lenses", *Light Sci. Appl*. no. 7, p. 17162, 2018. doi:10.1038/lsa.2017.162

[3] W. Xu, W. Xu, N. Bouet, *et al*. "2D MEMS-based multilayer Laue lens nanofocusing optics for high-resolution hard x-ray microscopy", *Opt. Express*, vol. 28, no. 12, pp. 17660-17771, 2020. doi:10.1364/OE.389555

[4] S. Takagi, "Dynamical Theory of Diffraction Applicable to Crystals with Any Kind of Small Distortion", *Acta. Crystallogr.,* pp. 1311-1312, Dec. 1962.

[5] S. Yue, L. Zhou, Y. Yang, *et al*., "Hard X-ray focusing resolution and efficiency test with a thickness correction multilayer Laue lens", *Nucl. Sci. Tech.*, vol. 33, p. 118, 2022. doi:10.1007/s41365-022-01102-1

[6] S. Yue, L. Zhou, M. Li, *et al*., "Calculated performance of multilayer Laue lens based on actual layer thickness and coupled wave theory", *Opt. Eng*, vol. 60, no. 9, p. 094111, Sep. 2021. doi:10.1117/1.OE.60.9.094111
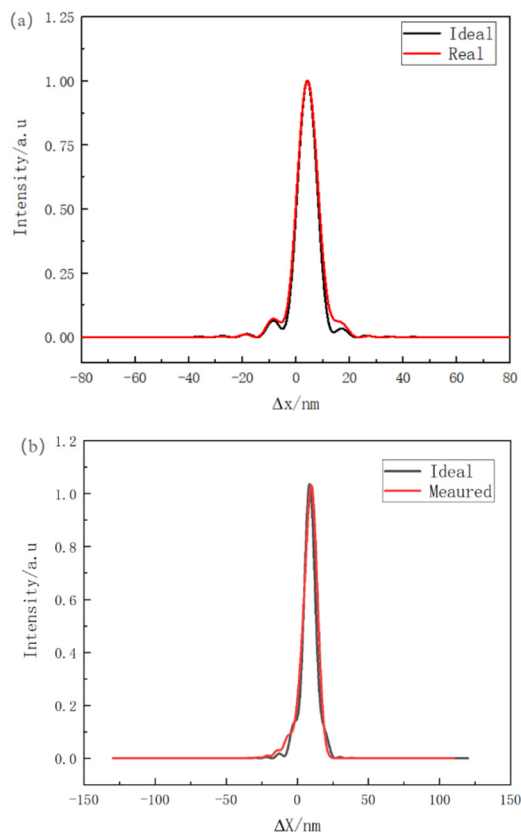
Figure 9: The intensity distribution of HMLL (a) and VMLL (b).